OPTICS

Nanoscale optical pulse limiter enabled by refractory metallic quantum wells

Haoliang Qian[1]*, Shilong Li[1]*, Yingmin Li[2], Ching-Fu Chen[1], Wenfan Chen[2], Steven Edward Bopp[2], Yeon-Ui Lee[1], Wei Xiong[2,3], Zhaowei Liu[1,2,4†]

The past several decades have witnessed rapid development of high-intensity, ultrashort pulse lasers, enabling deeper laboratory investigation of nonlinear optics, plasma physics, and quantum science and technology than previously possible. Naturally, with their increasing use, the risk of accidental damage to optical detection systems rises commensurately. Thus, various optical limiting mechanisms and devices have been proposed. However, restricted by the weak optical nonlinearity of natural materials, state-of-the-art optical limiters rely on bulk liquid or solid media, operating in the transmission mode. Device miniaturization becomes complicated with these designs while maintaining superior integrability and controllability. Here, we demonstrate a reflection-mode pulse limiter (sub–100 nm) using nanoscale refractory films made of Al_2O_3/TiN/Al_2O_3 metallic quantum wells (MQWs), which provide large and ultrafast Kerr-type optical nonlinearities due to the quantum size effect of the MQW. Functional multilayers consisting of these MQWs could find important applications in nanophotonics, nonlinear optics, and meta-optics.

INTRODUCTION

An optical limiter allows linear transmission/reflection below a certain incident light intensity or power threshold; above that threshold, the device keeps the transmitted/reflected optical power below a specified, tunable value (*1*, *2*). The use of an appropriate limiter in front of an optical sensor, thus, not only protects the sensor but also extends its working range to conditions more severe than previously thought possible. In contrast to the complicated, actively controlled optical limiting systems, passive optical limiters have a fast response time and are widely used to limit short optical pulses (*1*). These passive optical limiters use materials that have one of the following nonlinear optical properties: nonlinear refraction (self-focusing or defocusing) (*1*–*3*), nonlinear absorption (reverse saturable absorption or multiple-photon absorption) (*2*, *4*–*9*), or nonlinear scattering (microbubbles or microplasmas) (*10*–*12*). Since most of these nonlinear processes are based on the optical Kerr effect, which gives an ultrafast response time (on the order of one electronic orbital period, approximately 10^{-16} s) (*13*), extraordinary Kerr-type nonlinear materials have become a crucial element for new passive optical limiters to protect against ultrashort optical pulses.

A material's Kerr nonlinearity is a third-order correction to its linear optical response and is therefore extremely weak (*13*). Consequently, to provide a long interaction length for accumulating sufficient nonlinearity, Kerr-type passive optical limiters are typically made using macroscale solid or liquid media shown in Fig. 1 (A and B). The necessity of an additional intermediate focal plane (*3*) and difficult fabricating of inhomogeneously distributed nonlinear media (*6*) of these bulk limiting devices have become disappointing shortcomings of conventional optical limiters. To this end, optically resonant structures could be helpful; for example, an emerging reflective optical limiter based on resonant transmission has been demonstrated (*14*), which limits high-intensity transmission by enhancing the reflection (Fig. 1C). Nevertheless, this optical limiter still works in the transmission mode and is thick (5 to 6 μm) to maintain a high-quality narrow-band cavity mode. If possible, these drawbacks could be overcome by a reflection-mode nanoscale optical limiter, such as that shown in Fig. 1D. However, there is no report on a material or materials system that can provide a strong enough Kerr nonlinearity in the nanoscale to enable such a reflection-mode pulse-limiting effect.

Recently, a giant Kerr nonlinearity, several orders larger than those of the traditional nonlinear materials (*15*), has been obtained in ultrathin Au films (~3 nm thick). This strong Kerr nonlinearity is attributed to the large intersubband dipole moment and a high free electron density in the metal; these effects can be described well by a metallic quantum well (MQW) model (*15*, *16*). However, Au is not a durable material for extreme light nonlinear optics, and resultantly, the enhanced Kerr nonlinearity in the Au MQW cannot be used for high-intensity ultrashort pulse limiters.

RESULTS

Here, we demonstrate a nanoscale Kerr-type optical limiter (sub–100 nm) for femtosecond pulses (refer to text S1 and fig. S1; see Materials and Methods) based on a durable MQW material system. It consists entirely of the refractory materials (*17*, *18*) TiN and Al_2O_3 and is thereby ideal for high-intensity nonlinear optical applications. A refractory MQW optical limiter was epitaxially grown on a sapphire substrate (refer to text S2 and fig. S2; see Materials and Methods) with atomic level accuracy. The MQW is formed by an Al_2O_3/TiN/Al_2O_3 sandwich structure where free electrons in the metallic well (TiN) are quantized between the neighboring dielectric barriers (Al_2O_3) (*19*). As a result, the electronic conduction band of the confined TiN nanofilm is split into subbands, similar to the case of Au MQWs. The calculated electronic band diagram of a single MQW unit (2-nm TiN), based on the quantum electrostatic model for quantum-sized metals

[1]Department of Electrical and Computer Engineering, University of California, San Diego, 9500 Gilman Dr., La Jolla, CA 92093, USA. [2]Materials Science and Engineering, University of California, San Diego, 9500 Gilman Dr., La Jolla, CA 92093, USA. [3]Department of Chemistry and Biochemistry, University of California, San Diego, 9500 Gilman Dr., La Jolla, CA 92093, USA. [4]Center for Memory and Recording Research, University of California, San Diego, 9500 Gilman Dr., La Jolla, CA 92093, USA.
*These authors contributed equally to this work.
†Corresponding author. Email: zhaowei@ucsd.edu

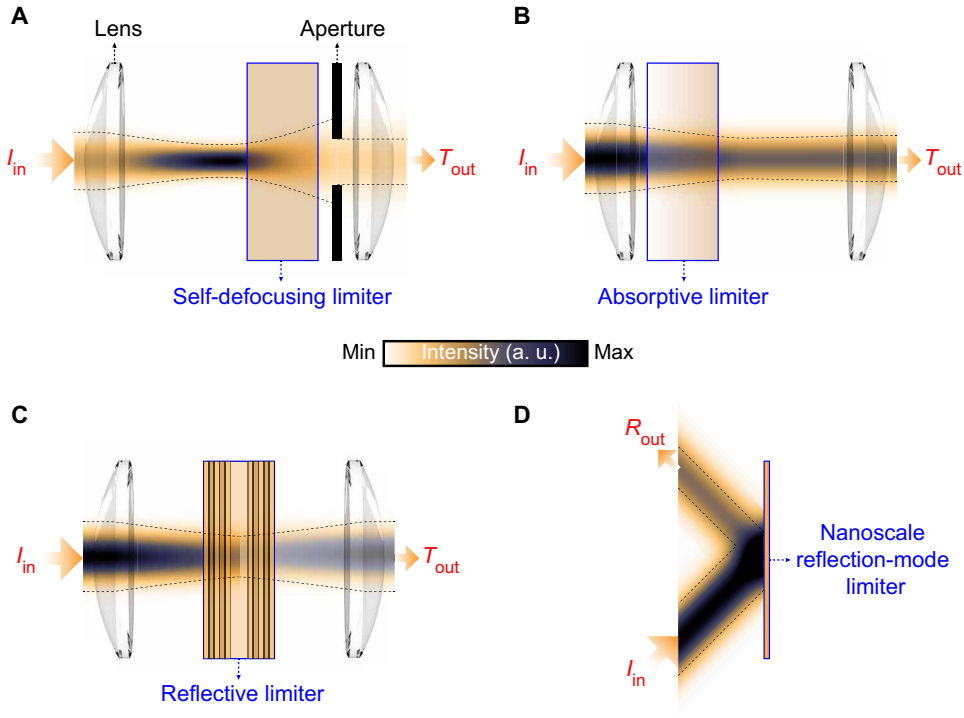

Fig. 1. Comparison of the traditional bulk transmission-mode and the proposed nanoscale reflection-mode pulse limiters. (**A** and **B**) Conventional configurations (not to scale) widely used for optical limitation based on Kerr-induced self-defocusing (A) and Kerr-type nonlinear absorption (such as TPA) (B). The former is achieved by inserting a bulk Kerr medium behind the focal plane to accelerate the divergence of an incident Gaussian beam with a high intensity so that only a fraction of the beam is allowed to pass through a preassigned aperture. The latter is performed by placing a bulk Kerr medium ahead of the focal plane to absorb the incident beam's high-intensity portion. Note that an inhomogeneously distributed bulk Kerr medium, as shown in (B), is desired to maximize the nonlinear absorption. (**C**) Recently emerging reflective optical limiter (not to scale). To limit the high-intensity transmission, instead of increasing the absorption (B), the reflection of the reflective pulse limiter will be enhanced because of off-resonance above the threshold intensity. (**D**) Schematic representation of the nanoscale reflective optical limiter (not to scale). The deeply subwavelength optical limiter film can be integrated onto the surface of an existing optical component.

(*15*, *16*), is shown in Fig. 2A, together with the dispersion of the subbands (refer to text S3). It is shown that the first five subbands are below the Fermi level, and thus, there would be a wealth of electronic transitions. As will be discussed later, these transitions contribute to the pulse-limiting effect via the Kerr nonlinearity of the MQW intersubband system, as well as various multiple-photon absorption processes. Therefore, it is the plentiful electronic subbands that enable the unprecedented pulse-limiting behavior of the nanoscale refractory thin films.

The MQW samples exhibit a metal-like high reflection at low-intensity illumination due to the plasmonic effect of TiN (*17*). To investigate the intrinsic nonlinear coefficient $\boldsymbol{n}_2$, samples with a single MQW unit were used for the z-scan measurement (*20*) (refer to text S4 and fig. S3), and the result is summarized in Fig. 2B. A resolved resonant peak is observed, which is associated with the single-photon transition (Kerr nonlinearity) between subbands $|2\rangle$ and $|3\rangle$, agreeing with the calculated electronic band structure (Fig. 2A). The amplitude of $\boldsymbol{n}_2$ is several orders larger than those of the traditional nonlinear materials (*13*), which is a direct evidence of electron subbands resulting from the quantum size effect in the MQW (*15*, *21*). Such high $\boldsymbol{n}_2$ makes these devices suitable for nonlinear optical applications including the optical limiter. Moreover, the sign of the real part of $\boldsymbol{n}_2$ is positive, while that of its imaginary part is negative. As a result, the MQW would turn out to be a dielectric at high-intensity illumination. For this reason, the proposed optical limiter based on this MQW system works in a reflection mode, i.e., it allows a linear reflection for incident light with intensity below the limiting threshold, while above the limiting threshold, it keeps the reflected optical power below a certain tunable value. To the best of our knowledge, it is the first reflection-mode optical limiter; this advancement gives a new degree of freedom for the optimal design of an optical limiting system.

Distinctly different from conventional optical limiters, the nanoscale MQW thin film for a femtosecond pulse limiter works in the reflection mode schematically shown in Fig. 3A. As a consequence, it can be integrated onto the surface of an existing optical component down to subwavelength scale, significantly simplifying the optical limiting configuration. We initially design the quantum well thickness such that there would be one or a few intersubband transitions at the desired working frequency range. In addition, to ensure a sufficient interaction length for the Kerr response to support a reasonable pulse-limiting effect, a stack of quantum wells forming an effective metamaterial are needed to improve its performance (*22*). Note that the barrier layer cannot be too thin to avoid the unwanted tunneling effect between quantum wells. Here, the sample composed of 7-unit MQW was fabricated and used in the pulse-limiting experiments as the case demonstration; additional consideration is paid to the sample quality and the fabrication complexity as well. Note that the periodicity of 7 for the multiple MQW films naturally manifests itself as metamaterials (*23*). As discussed later, the marked decrease in the

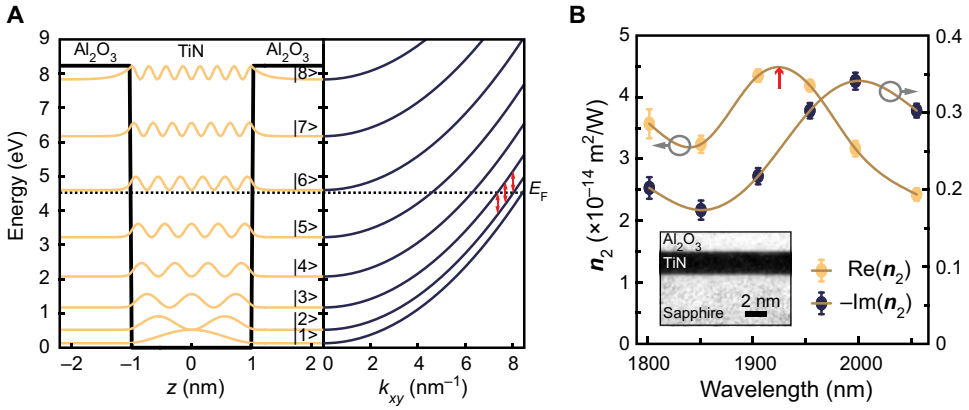

Fig. 2. Multiple electronic subbands in the quantum-sized TiN films enabling extraordinarily high Kerr coefficients. (**A**) Conduction band diagram of a TiN MQW (left) and the corresponding electronic dispersion of subbands (right). The Fermi level E_F (~4.6 eV) is shown as the dashed line. The red arrows indicate the single-photon intersubband transitions between subbands $|2\rangle$ and $|3\rangle$. (**B**) Wavelength dependence of the nonlinear optical constant $\boldsymbol{n}_2$ of a 2-nm-thick TiN film, measured by the z-scan technique using 45°-incident *p*-polarized laser pulses (100-fs pulse width, 1-kHz repetition rate; Astrella, Coherent) with the intensity of ~70 GW/cm^2. Note that a minus "−" is used in the imaginary party of the $\boldsymbol{n}_2$. The red arrow corresponds to the calculated transition wavelength shown in (A), while the solid lines are the spline-fitted curves. The fluctuations in multiple measurements at various locations are indicated by the error bars (SD). Inset shows a typical transmission electron microscopy (TEM) cross-section of a TiN MQW thin film.

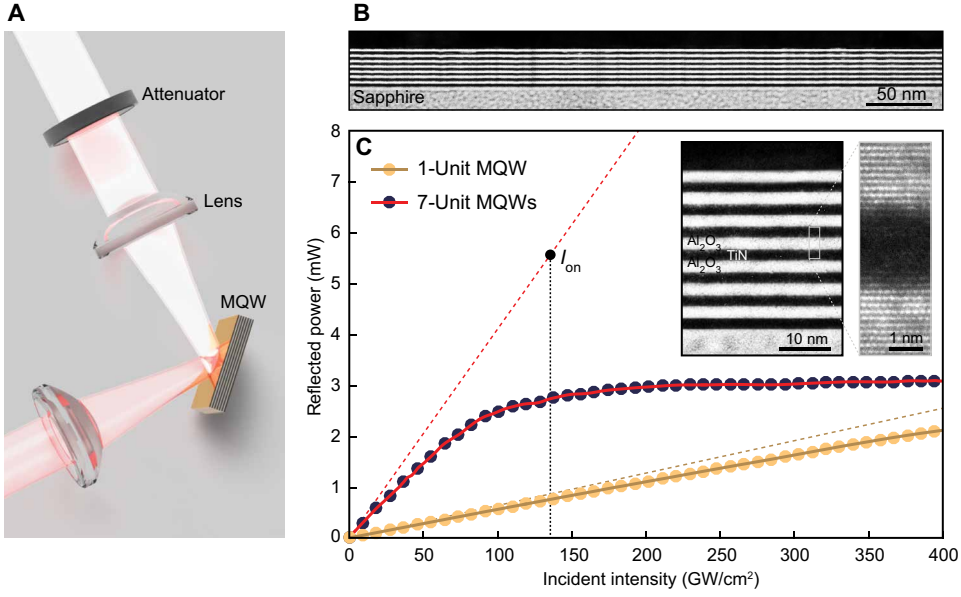

Fig. 3. Experimental demonstration of the reflection-mode nanoscale femtosecond pulse limiter using TiN-based MQWs. (**A**) Experimental configuration of the reflection-mode pulse limiter (not to scale). The attenuator is used to vary the incident powers for obtaining pulse-limiting curves. (**B**) Typical TEM cross section of a 7-unit MQW thin film. The layer on top of the MQWs is a protective layer used only for TEM cross section preparation during the focused ion beam cutting process. (**C**) Intensity dependence of the measured reflected power for samples with a single unit and 7 units of MQW at the wavelength of 1997 nm (100-fs pulse width, 1-kHz repetition rate, 130-μm beam radius, 45° incidence, and *p* polarization). The dashed lines show the corresponding linear reflection curves. The onset-of-limiting intensity I_{on} is defined in the main text. Insets show a zoomed-in TEM cross section of the 7-unit MQW thin film (left) and a dark-field high-resolution TEM image (right) showing the high quality of the grown multilayer.

imaginary part of refractive index (*14*) is critical for both improving the pulse-limiting performance and ensuring the device's thermal durability, due to the large negative imaginary part of $\boldsymbol{n}_2$ in the Kerr-type metamaterials (*22*) (see the z-scan result for the 7-unit MQW sample in fig. S3). Note also that the epitaxial growth capability of the refractory plasmonic metal TiN on sapphire substrates (*24*) enables MQW heterostructures with atomic-level accuracy (see Fig. 3B and the insets of Fig. 3C), which further increases their thermal durability and is thus superior to the Au-based MQW system (*15*, *16*). Figure 3C depicts the intensity-dependent reflected power at 1997-nm wavelength (see the wavelength dependence of the pulse limiting in text S5 and fig. S4) for samples with a single unit, and 7 units of the MQW, respectively. In keeping with the implications of optical limitation, there is a nearly linear reflection below a certain intensity threshold, and above it, the reflected power saturates to a certain value for the 7-unit MQW sample, while the single-unit sample shows a

weak pulse-limiting effect in the intensity range due to the limited thickness and interaction length. This unprecedented tunability gained solely by stacking MQWs renders the nanoscale pulse limiters versatile, a crucial element in the design of compact optical and photonic systems.

In analogy to the conventional pulse limiter working in a transmission mode (*3*), several parameters for the proposed reflection-mode pulse limiter can be defined (see Fig. 3C). In no particular order, these are linear reflectivity, onset-of-limiting intensity, dynamic range (DR), and reflectivity just before the maximum safe limitation intensity (SLI; refer to text S6). Linear reflectivity R_{lin} is desired to be as high as possible. The onset-of-limiting intensity I_{on}, which is ideally tunable, is defined as the incident intensity at which the reflectivity R drops off to $R_{lin}/2$. DR is the third parameter and defined as $(I_{SLI} - I_{on})/I_{on}$, where I_{SLI} is the SLI of the MQW samples, whose maximum, in this case, was determined experimentally to be 400 GW/cm^2 (refer to text S6 and figs. S5 and S6). Larger DR it is, longer operating intensity range the pulse limiter supports. Last, reflectivity just before the SLI, R_{SLI}, is desired to be as low as possible. The wavelength dependence of these parameters is listed in Table 1. It is to emphasize that, by means of metamaterial-enabled engineering (refer to text S7 and fig. S7), the thickness of the nanoscale MQW films provides an extraordinary tunability of the pulse-limiting performance compared with those of the bulk optical limiters.

The $\boldsymbol{n}_2$ obtained by the z-scan technique using a moderate-intensity laser pulse shows a large Kerr nonlinearity provided by the MQW. However, $\boldsymbol{n}_2$ is dependent on the optical intensity, especially under high-intensity illumination when the optical limiting effect is activated. Therefore, to study high-intensity nonlinearities, the reflectivity and transmissivity for 1997-nm laser pulses (100-fs pulse width, 1-kHz repetition rate, and 130-μm beam radius) with various intensities up to the SLI (400 GW/cm^2) were measured (refer to text S8 and fig. S8) and then used to extract the intensity-dependent optical constant $\boldsymbol{n}_I$ [$\boldsymbol{n}_I = \boldsymbol{n}_0 + \boldsymbol{n}_{2(I)}I$] for a given intensity I. The results for the sample with 7 units of MQW are summarized in Fig. 4A. As can be seen, the real part of $\boldsymbol{n}_I$, Re($\boldsymbol{n}_I$), quickly increases and saturates before entering the high-intensity range and then drops, while its imaginary part, Im($\boldsymbol{n}_I$), decreases to almost 0 as the intensity increases, it then slowly increases to a small value at high intensity. Both the marked increase in Re($\boldsymbol{n}_I$) and decrease in Im($\boldsymbol{n}_I$) quickly turn the MQW from a metal to a dielectric, enabling the pulse-limiting effect and also sustaining the MQW samples under a high intensity with a low absorption rate [the small Im($\boldsymbol{n}_I$)]. Maximum changes of ~65 and ~100%, respectively, in the real and imaginary parts of $\boldsymbol{n}_I$ are obtained, which again reveal the large Kerr nonlinearities in the MQW. In addition, the metal/dielectric transition (around the intensity of 4 GW/cm^2) is clearly visible in Fig. 4A, as expected.

As mentioned above, the strong Kerr response of MQWs originates from the single-photon transition between the subbands $|2\rangle$ and $|3\rangle$. In addition, it will be saturated because of the concomitant single-photon absorption (1PA) and two-photon absorption (TPA) processes, which can be described by the absorption saturation model (*25*). The 1PA is associated with the intersubband transition from subbands $|2\rangle$ to $|3\rangle$ (see the inset of Fig. 4B), and it will be saturated above a certain intensity. The whole 1PA saturation process can be modeled (*13*, *25*) by an intensity-dependent absorption coefficient $\alpha_I = \alpha_0/(1 + I/I_{sat,1PA})$, where λ, α_0, and $I_{sat,1PA}$ are, respectively, the wavelength of incident light, the 1PA coefficient constant, and the saturation intensity of 1PA. Similarly, the TPA from subbands $|5\rangle$ to $|6\rangle$ (see the inset in Fig. 4B) can also be modeled (*25*) via the intensity-dependent absorption coefficient $\beta_I = \beta_0/(1 + (I/I_{sat,\,TPA})^2)$, where β_0 and $I_{sat,\,TPA}$ are, respectively, the TPA coefficient constant and saturation intensity. Therefore, the imaginary part of $\boldsymbol{n}_I$ in the entire intensity range is well fitted by the relation of $\mathrm{Im}(\boldsymbol{n}_I) = \lambda(\alpha_I + \beta_I I)/(4\pi)$, as shown in Fig. 4B (refer to text S9).

Because of both the 1PA and TPA, free electrons above the Fermi sea are continuously promoted. These promoted hot electrons above the Fermi sea can be described by the Drude model and, thus, induce a negative change Δn_I (*26*, *27*) in the real part of $\boldsymbol{n}_I$ (i.e., $\Delta n_I \propto -N_{hot}$, where N_{hot} is the density of the hot electrons), pulling down the real

Table 1. Wavelength dependence of performance parameters for the nanoscale thin-film pulse limiter with 7 units of MQW.

λ (nm)	R_{lin}	I_{on} (GW/cm^2)	DR	R_{SLI}
1802	31.7%	96	317%	8.9%
1905	31.8%	162	147%	9.0%
1997	32.3%	132	202%	6.8%

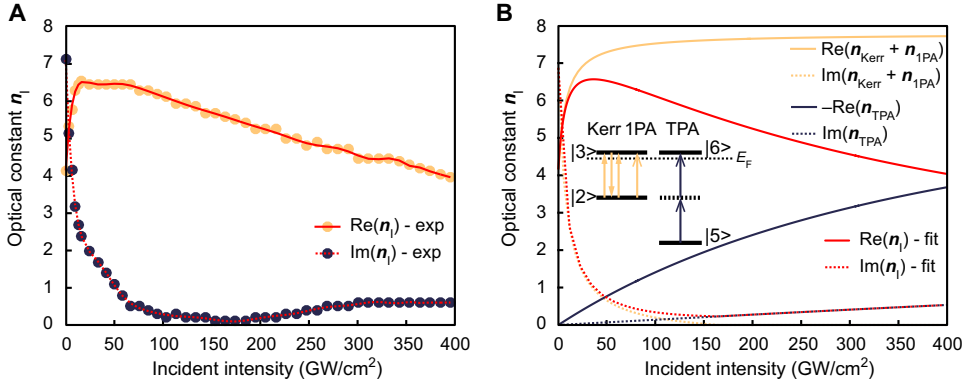

Fig. 4. Physics of optical Kerr nonlinearities of the MQWs. (**A** and **B**) Intensity-dependent refractive index $\boldsymbol{n}_I$ extracted from the experimentally measured reflectivity and transmissivity ["exp" in (A)] and fitted by the single-photon absorption (1PA) and two-photon absorption (TPA) saturation models ["fit" in (B)]. Inset of (B) shows diagrams representing the Kerr, 1PA, and TPA processes, respectively. The sample used has 7 units of MQW, and the data are taken at the wavelength of 1997 nm.

part of n_I at high intensity. Combining the 1PA and TPA saturation models and the Drude model, the real part of n_I is well fitted (Fig. 4B and see details in text S9).

DISCUSSION

The nanoscale pulse-limiting MQW thin film demonstrated in the 1.8- to 2-μm spectral range is readily accessible by the optical system supplied by the compact and efficient high-power diode lasers emitting at wavelengths from 1.8 to 2.3 μm for their wide range of applications (*28*). We believe that, because of the multiple intersubband transitions and their broadband Kerr effect in MQW systems (*15*), it would have similar pulse-limiting performance in the near-infrared (near-IR) wavelengths from 1 to 1.8 μm via the corresponding intersubband transitions.

CONCLUSION

In conclusion, we have demonstrated a nanoscale reflection-mode femtosecond pulse-limiting thin film made of refractory materials. It is enabled by the large and ultrafast optical Kerr nonlinearities of the embedded MQWs. These unprecedented intensity-dependent Kerr nonlinearities are attributed to the plentiful electron subbands in the MQW, providing a new mechanism for engineering extraordinary optical nonlinearities and novel applications. Further efforts on the tunability of the nontrivial optical limiting, e.g., the working wavelength range and the working intensity range, could be made with the thin film consisting of different thicknesses of single MQW or coupled MQWs (*29*, *30*). Further functionalization and integration of the nanoscale pulse-limiting MQW thin film would enable numerous applications in nonlinear optics and integrated photonics.

MATERIALS AND METHODS

Sample growth

MQWs made of refractory materials (TiN and Al_2O_3) were grown by the magnetron sputtering technique (AJA International) on sapphire substrates (*31*). The reactive growth temperature of TiN was set as 350°C with an N_2/Ar gas ratio of 7:3. The Al_2O_3 was deposited by sputtering in the same chamber as the TiN growth. Deposition ambiance is given as the follows: An Al_2O_3 target was used; the temperature for the Al_2O_3 growth was set as 350°C, the same as for the growth of TiN; the growth power is 150 W with 5 sccm Ar under 5-mT pressure; and the growth speed is about 0.4 nm/min.

Laser pulse duration characterization

The Coherent Astrella laser system was used to generate 50-fs pulses with a 792-nm center wavelength, which were directed to pump an optical parametric amplifier (TOPAS-Prime, Light Convesion) to generate ultrafast tunable near-IR pulses. A light beam with the desired near-IR wavelength was selected as the output for the following characterization and pulse-limiting experiments. The pulse duration of the selected unfocused near-IR beam was measured by a home-built single-shot autocorrelator (*32*). It was projected onto the spatial mode of second harmonic generation (SHG) between two crossed near-IR beams, which was measured by a line camera. The measured pulse duration of the unfocused near-IR beam is around 87 fs. In the following z-scan and pulse-limiting experiments, a focal lens was used, so the estimated pulse duration was 90 to 100 fs.

SUPPLEMENTARY MATERIALS

Supplementary material for this article is available at http://advances.sciencemag.org/cgi/content/full/6/20/eaay3456/DC1

REFERENCES AND NOTES

1. L. W. Tutt, T. F. Boggess, A review of optical limiting mechanisms and devices using organics, fullerenes, semiconductors and other materials. *Prog. Quant. Electron.* **17**, 299–338 (1993).
2. G.-J. Zhou, W.-Y. Wong, Organometallic acetylides of Pt^{II}, Au^{I} and Hg^{II} as new generation optical power limiting materials. *Chem. Soc. Rev.* **40**, 2541–2566 (2011).
3. A. Nevejina-Sturhan, O. Werhahn, U. Siegner, Low-threshold high-dynamic-range optical limiter for ultra-short laser pulses. *Appl. Phys. B* **74**, 553–557 (2002).
4. S. Hirata, K. Totani, T. Yamashita, C. Adachi, M. Vacha, Large reverse saturable absorption under weak continuous incoherent light. *Nat. Mater.* **13**, 938–946 (2014).
5. G.-K. Lim, Z.-L. Chen, J. Clark, R. G. S. Goh, W.-H. Ng, H.-W. Tan, R. H. Friend, P. K. H. Ho, L.-L. Chua, Giant broadband nonlinear optical absorption response in dispersed graphene single sheets. *Nat. Photonics* **5**, 554–560 (2011).
6. J. W. Perry, K. Mansour, I.-Y. S. Lee, X.-L. Wu, P. V. Bedworth, C.-T. Chen, D. Ng, S. R. Marder, P. Miles, T. Wada, M. Tian, H. Sasabe, Organic optical limiter with a strong nonlinear absorptive response. *Science* **273**, 1533–1536 (1996).
7. L. W. Tutt, A. Kost, Optical limiting performance of C_{60} and C_{70} solutions. *Nature* **356**, 225–226 (1992).
8. B. Zhao, B. Cao, W. Zhou, D. Li, W. Zhao, Nonlinear optical transmission of nanographene and its composites. *J. Phys. Chem. C* **114**, 12517–12523 (2010).
9. Q. Li, C. Liu, Z. Liu, Q. Gong, Broadband optical limiting and two-photon absorption properties of colloidal GaAs nanocrystals. *Opt. Express* **13**, 1833–1838 (2005).
10. K. Mansour, M. J. Soileau, E. W. Van Stryland, Nonlinear optical properties of carbon-black suspensions (ink). *J. Opt. Soc. Am. B* **9**, 1100–1109 (1992).
11. K. M. Nashold, D. P. Walter, Investigations of optical limiting mechanisms in carbon particle suspensions and fullerene solutions. *J. Opt. Soc. Am. B* **12**, 1228–1237 (1995).
12. L. Vivien, D. Riehl, J.-F. Delouis, J. A. Delaire, F. Hache, E. Anglaret, Picosecond and nanosecond polychromatic pump–probe studies of bubble growth in carbon-nanotube suspensions. *J. Opt. Soc. Am. B* **19**, 208–214 (2002).
13. R. W. Boyd, *Nonlinear Optics* (Academic Press, ed. 3, 2008).
14. J. H. Vella, J. H. Goldsmith, A. T. Browning, N. I. Limberopoulos, I. Vitebskiy, E. Makri, T. Kottos, Experimental realization of a reflective optical limiter. *Phys. Rev. Appl.* **5**, 064010 (2016).
15. H. Qian, Y. Xiao, Z. Liu, Giant Kerr response of ultrathin gold films from quantum size effect. *Nat. Commun.* **7**, 13153 (2016).
16. H. Qian, Y. Xiao, D. Lepage, L. Chen, Z. Liu, Quantum electrostatic model for optical properties of nanoscale gold films. *Nanophotonics* **4**, 413–418 (2015).
17. U. Guler, A. Boltasseva, V. M. Shalaev, Refractory plasmonics. *Science* **344**, 263–264 (2014).
18. W. Li, U. Guler, N. Kinsey, G. V. Naik, A. Boltasseva, J. Guan, V. M. Shalaev, A. V. Kildishev, Refractory plasmonics with titanium nitride: Broadband metamaterial absorber. 26, 7959–7965 (2014).
19. H. Qian, S. Li, C.-F. Chen, S.-W. Hsu, S. E. Bopp, Q. Ma, A. R. Tao, Z. Liu, Large optical nonlinearity enabled by coupled metallic quantum wells. *Light Sci. Appl.* **8**, 13 (2019).
20. M. Sheik-Bahae, A. A. Said, T. H. Wei, D. J. Hagan, E. W. V. Stryland, Sensitive measurement of optical nonlinearities using a single beam. *IEEE J. Quantum Electron.* **26**, 760–769 (1990).
21. J. B. Khurgin, S. Li, Two-photon absorption and nonresonant nonlinear index of refraction in the intersubband transitions in the quantum wells. *Appl. Phys. Lett.* **62**, 126–128 (1993).
22. A. D. Neira, N. Olivier, M. E. Nasir, W. Dickson, G. A. Wurtz, A. V. Zayats, Eliminating material constraints for nonlinearity with plasmonic metamaterials. *Nat. Commun.* **6**, 7757 (2015).
23. R. Liu, T. J. Cui, D. Huang, B. Zhao, D. R. Smith, Description and explanation of electromagnetic behaviors in artificial metamaterials based on effective medium theory. *Phys. Rev. E Stat. Nonlin. Soft Matter. Phys.* **76**, 026606 (2007).
24. G. V. Naik, B. Saha, J. Liu, S. M. Saber, E. A. Stach, J. M. K. Irudayaraj, T. D. Sands, V. M. Shalaev, A. Boltasseva, Epitaxial superlattices with titanium nitride as a plasmonic component for optical hyperbolic metamaterials. *Proc. Natl. Acad. Sci. U.S.A.* **111**, 7546–7551 (2014).
25. G. S. He, Q. Zheng, A. Baev, P. N. Prasad, Saturation of multiphoton absorption upon strong and ultrafast infrared laser excitation. *J. Appl. Phys.* **101**, 083108 (2007).
26. A. Brodeur, S. L. Chin, Ultrafast white-light continuum generation and self-focusing in transparent condensed media. *J. Opt. Soc. Am. B* **16**, 637–650 (1999).
27. E. Yüce, G. Ctistis, J. Claudon, E. Dupuy, K. J. Boller, J.-M. Gérard, W. L. Vos, Competition between electronic Kerr and free-carrier effects in an ultimate-fast optically switched semiconductor microcavity. *J. Opt. Soc. Am. B* **29**, 2630–2642 (2012).
28. M. T. Kelemen, J. Gilly, M. Haag, J. Biensenbach, M. Rattunde, J. Wagner, Diode laser arrays for 1.8 to 2.3 μm wavelength range, in *Proceedings of SPIE OPTO: Integrated Optoelectronic Devices* (SPIE, 2009), vol. 7230, pp. 9.

29. E. Rosencher, A. Fiore, B. Vinter, V. Berger, P. Bois, J. Nagle, Quantum engineering of optical nonlinearities. *Science* **271**, 168–173 (1996).
30. J. Lee, M. Tymchenko, C. Argyropoulos, P.-Y. Chen, F. Lu, F. Demmerle, G. Boehm, M.-C. Amann, A. Alù, M. A. Belkin, Giant nonlinear response from plasmonic metasurfaces coupled to intersubband transitions. *Nature* **511**, 65–69 (2014).
31. P. Patsalas, N. Kalfagiannis, S. Kassavetis, Optical properties and plasmonic performance of titanium nitride. *Materials* **8**, 3128–3154 (2015).
32. F. Salin, P. Georges, G. Roger, A. Brun, Single-shot measurement of a 52-fs pulse. *Appl. Optics* **26**, 4528–4531 (1987).
33. G. V. Naik, J. Kim, A. Boltasseva, Oxides and nitrides as alternative plasmonic materials in the optical range. *Opt. Mater. Express* **1**, 1090–1099 (2011).
34. E. Rosencher, B. Vinter, *Optoelectronics* (Cambridge Univ. Press, 2002).
35. B. C. Stuart, M. D. Feit, S. Herman, A. M. Rubenchik, B. W. Shore, M. D. Perry, Optical ablation by high-power short-pulse lasers. *J. Opt. Soc. Am. B* **13**, 459–468 (1996).

Acknowledgments
Funding: We acknowledge financial support from the NSF–Division of Materials Research (grant no. 1610538) and the DARPA DSO-NLM Program (grant no. HR00111820038). Y.L. and W.X. thank support from the DARPA YFA program (grant no. D15AP000107). S.L. acknowledges the financial support of the International Postdoctoral Exchange Fellowship Program (no. 20170010). **Author contributions:** H.Q. and Z.L. conceived the idea. S.L. and H.Q. performed the theoretical calculation and numerical simulation. H.Q. performed the sample growth. H.Q., Y.L. and C.-F.C. performed the experiments. W.C. performed the laser system characterization. S.L., H.Q., S.E.B., and Z.L. wrote the manuscript. All authors analyzed the data and revised the manuscript. Z.L. supervised the research. **Competing interests:** The authors declare that they have no competing interests. **Data and materials availability:** All data needed to evaluate the conclusions in the paper are present in the paper and/or the Supplementary Materials. Additional data related to this work may be requested from the authors.

Submitted 11 June 2019
Accepted 28 February 2020
Published 15 May 2020
10.1126/sciadv.aay3456

Citation: H. Qian, S. Li, Y. Li, C.-F. Chen, W. Chen, S. E. Bopp, Y.-U. Lee, W. Xiong, Z. Liu, Nanoscale optical pulse limiter enabled by refractory metallic quantum wells. *Sci. Adv.* **6**, eaay3456 (2020).

ScienceAdvances

Nanoscale optical pulse limiter enabled by refractory metallic quantum wells

Haoliang Qian, Shilong Li, Yingmin Li, Ching-Fu Chen, Wenfan Chen, Steven Edward Bopp, Yeon-Ui Lee, Wei Xiong and Zhaowei Liu

Sci Adv **6** (20), eaay3456.
DOI: 10.1126/sciadv.aay3456